

(1969).

⁸J. Bardeen, L. N. Cooper, and J. R. Schrieffer, Phys. Rev. **108**, 1175 (1957).⁹P. Rhodes, Proc. Roy. Soc. (London) **A204**, 396 (1950).¹⁰P. G. Klemens and L. Tewordt, Rev. Mod. Phys. **36**, 118 (1964).¹¹J. E. Gueths, N. N. Clark, D. Markowitz, F. V. Burckbuchler, and C. A. Reynolds, Phys. Rev. **163**, 364

(1967).

¹²P. L. Garbarino and C. A. Reynolds, Phys. Rev. (to be published).¹³G. J. Pearson, C. W. Ulbrich, J. E. Gueths, M. A. Mitchell, and C. A. Reynolds, Phys. Rev. **154**, 329 (1967).¹⁴J. E. Gueths, F. V. Burckbuchler, and C. A. Reynolds, Rev. Sci. Instr. **40**, 1344 (1969).

PHYSICAL REVIEW B

VOLUME 2, NUMBER 9

1 NOVEMBER 1970

Current-Pulse Effect in the Intermediate State of Superconducting Lead Films*

R. P. Huebener

Argonne National Laboratory, Argonne, Illinois 60439

(Received 9 February 1970)

The enhancement of the resistive voltage in the intermediate state of superconducting lead films due to a high current pulse has been studied at 4.2°K as a function of the width of the pulse τ , the magnetic field H , and the film thickness. The film thickness ranged between 1 and 7 μm . The resistive voltage increment after the current pulse, plotted versus τ , yields S-shaped curves which saturate at high values of τ . The half-time τ^* decreases strongly with increasing H . Assuming that the voltage increment is caused by the formation of a laminar flux structure perpendicular to the current during the pulse, the product of τ^* and the flux-flow velocity v_ϕ during the pulse can be expected to be of the order of the periodicity length of the laminar flux structure. Estimating v_ϕ at the pulse current from the flux-flow resistivity at small currents, the product $\tau^* \times v_\phi$ increases with increasing film thickness and is in reasonable agreement with the value expected from Landau's model of the intermediate state. The current-pulse effect disappears below a film thickness between 1 and 2 μm . This can be understood from the experiments of Cody and Miller, which suggest that below a film thickness of about 1.5 μm lead films behave like type-II material.

INTRODUCTION

The electrical resistance in the intermediate state of type-I superconductors, in general, consists of two contributions: the Ohmic resistance within the normal regions and the flux-flow resistance due to the motion of the normal regions. The importance of flux-tube motion for the electrical resistance in the intermediate state has been demonstrated convincingly in recent experiments on the Ettingshausen^{1,2} and Nernst effect,^{3,4} and magnetic coupling,^{5,6} and in the visual observation of the motion of the flux structure in the presence of an electrical current.^{6,7} Further evidence for flux flow in type-I superconductors has been obtained from measurements of the noise voltage associated with a current.⁸ The relative contribution of both terms to the electrical resistance depends on the arrangement of the flux structure in the intermediate state. As one approaches the critical field, the contribution from flux flow becomes less and less important. The arrangement of the flux structure in the intermediate state can be changed strongly by an electrical current. Passing a high current through the specimen results in the formation of a laminar flux structure in which the laminae are oriented predom-

inantly perpendicular to the current direction.^{6,9}

The formation of this laminar structure leads to a hysteresis in the electrical resistance. Such a hysteresis has been reported first by Andrew¹⁰ and has been studied in detail recently by Solomon.⁶ In these experiments, the voltage was measured as a function of current while the current was raised from zero to a high value and then returned to zero. Recently, we have reported a current induced enhancement of the resistive voltage in the intermediate state of lead films using a somewhat different approach.¹¹ We have measured the voltage-current curves for relatively small currents before and after a pulse of high current had been passed through the specimen. A high-current pulse was found to cause an appreciable enhancement of the resistive voltage indicating a permanent rearrangement of the flux structure probably towards a laminar pattern perpendicular to the current.

A study of this current-pulse effect¹¹ as a function of the pulse width should indicate how the laminar pattern is gradually formed. From such measurements, knowing the flux-flow velocity during the current pulse, we can estimate the average distance each flux tube must travel to form the laminar pat-

tern. The flux-flow velocity during the pulse can be estimated from the flux-flow resistance (measured before a current pulse has been applied). With these ideas in mind we have studied the current-pulse effect in the intermediate state of superconducting lead films as a function of the width of the pulse τ , the magnetic field, and the film thickness. The increment in resistive voltage after the current pulse plotted versus τ was found to yield S-shaped curves which saturate at high values of τ . The distance traveled by the individual flux tubes during the rearrangement of the flux structure is estimated from these curves and the flux-flow velocity during the current pulse. It is found to be close to the periodicity length of the laminar flux structure expected from Landau's model of the intermediate state.

EXPERIMENTAL TECHNIQUE

The lead films were made by depositing 99.999% pure Pb from a Joule-heated tantalum boat on a glass microscope slide under a vacuum of about 1×10^{-6} Torr. The film width and the distance between the longitudinal voltage probes was 12 and 20 mm, respectively. The only exception was sample No. 33A, which was made from sample No. 33 by reducing the width to 7 mm. At the ends of the film, outside the gauge length, where the current leads were attached, the film width increased to 20 mm. The film thickness and the electrical resistance ratio $R(295 \text{ K})/R(4.2 \text{ K})$ [where $R(4.2)$ is measured in a magnetic field of 800 G perpendicular to the film] for the different samples are listed in Table I.

The electrical resistance was measured with the sample being in direct contact with the liquid-helium bath. The helium-bath temperature was always at 4.2 °K. A magnetic field perpendicular to the films was supplied by a superconducting solenoid.

In the earlier measurements,¹¹ a current pulse which decayed exponentially had been passed through the samples by discharging a capacitor. The present experiments were carried out with a rectangular pulse shape using a Hewlett Packard Model 214 A pulse generator. The pulse was monitored with an

oscilloscope. The generator supplied a current pulse with a maximum height of 2 A and a maximum width of 10 msec. Most experiments were done with a pulse height of about 1.9 A. For obtaining pulse times larger than 10 msec, a series of pulses with 10-msec width was applied.

The resistive voltages V were measured with the usual four-probe method. For measuring the enhancement of the resistive voltage as a function of the pulse width, the data were taken using the following sequence. The magnetic field was raised slowly from zero to the desired value taking care that no overshooting occurred. The resistive voltage was then measured, using a current value slightly above the critical current such that the voltage was in the range 0.1–0.5 μV . The measuring current was turned to zero and the current pulse (or a series of pulses) was applied. Then the measuring current was raised to its original value and the resistive voltage was remeasured. Before taking a new datum point, the magnetic field was returned to zero. By subtracting the voltage for zero current from the voltage readings, small thermoelectric voltages in the lead wires were eliminated. In addition to these data at one current value, some complete voltage-current curves before and after the current pulse were taken.

RESULTS AND DISCUSSION

In Fig. 1 we show the normalized electrical resistance of three samples at 4.2 °K versus the magnetic field perpendicular to the film. The resistance values of Fig. 1 were obtained from the linear region in the voltage-current curves above the critical current. At the critical field of each film, $H_C(\text{film})$, the resistance curves show a distinct bend. The location of these bends is indicated by the arrows in Fig. 1. The critical fields obtained from the location of the bend in the resistance curves such as shown in Fig. 1 are listed in Table I for the different samples. It is seen that the values of $H_C(\text{film})$ are clearly below the bulk critical field (550 G at 4.2 °K) and that they decrease with decreasing film thickness in the range investigated. Our values of $H_C(\text{film})$ obtained from the resistance and their dependence on film thickness are in good agreement with the data of Cody and Miller¹² for a perpendicular magnetic field.

Figure 2 shows an example of the enhancement of the resistive voltage after the application of a current pulse. The curve obtained without a current pulse has a fairly linear region below 400 mA and bends upwards at higher currents. Presumably, the bending of this curve at higher currents is due to a rearrangement of the flux structure induced by the current. Whereas all samples with a film thickness larger than 1 μm clearly showed an enhancement of the resistive voltage after the current pulse,

TABLE I. Sample Characteristics.

Sample No.	Film thickness (μm)	$\frac{R(295 \text{ K})}{R(4.2 \text{ K})}$	$H_C(\text{film})$ (G)	$v_e \times \tau^*$ (μm)
34	1.0	315	425	no pulse effect
35	2.3	618	450	0.6 ± 0.2
22	3.2	801	...	1.0
36	5.3	1153	475	1.7
33	6.5	1590	480	4
33A ^a	6.5	1656	...	4

^aSample No. 33 after width has been trimmed to 7 mm.

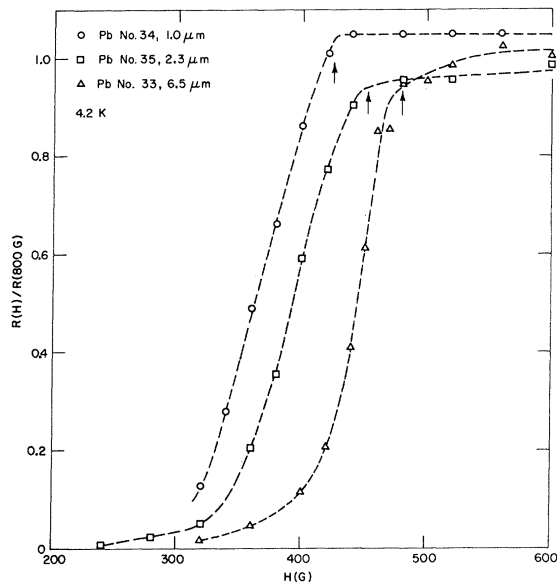


FIG. 1. Normalized electrical resistance of three specimens versus the magnetic field perpendicular to the film. The arrows indicate approximately the critical fields for the samples.

no such pulse effect could be detected in sample No. 34 with $1.0\text{ }\mu\text{m}$ film thickness. This absence of the current-pulse effect in the thinnest film of our series is very interesting and can be understood from the studies of the magnetic transitions in superconducting lead films by Cody and Miller.¹² These authors found that below a film thickness of about $1.5\text{ }\mu\text{m}$, lead films cease to behave like type-I material with a positive surface energy and show type-II behavior. If sample No. 34 does behave like type-II material, we cannot expect, of course, a flux structure consisting of large normal regions and therefore no current-pulse effect.

In Fig. 3 we show the resistive voltage enhancement due to the current pulse as a function of the pulse width for sample No. 22 at different magnetic fields. These data were taken with a pulse height of 1.9 A. The current values at which the voltages were measured before and after the pulse are listed in the figure. In Fig. 3 the difference of the voltage after and before the pulse divided by the voltage difference for a very long pulse is plotted versus the logarithm of the pulse width τ . As a function of τ , the voltage enhancement is seen to form S-shaped curves which saturate at high values of τ . The half-time τ^* at which the voltage enhancement reaches half its saturation value is indicated by the arrows in Fig. 3. We see that with increasing magnetic field τ^* decreases. In all samples showing the current-pulse effect the dependence of the voltage enhancement on τ was similar to that shown in Fig. 3.

The saturation of the voltage enhancement at high values of τ can be understood in terms of the formation of a laminar flux structure during the current pulse.^{6,9} With increasing τ , the flux tubes, present in the sample before the pulse, can travel farther and farther towards forming the laminar structure. After the laminar structure has been formed, no further change is expected with increasing τ . With this model, one pulse with the width τ should have the same effect as a series of n pulses with the width τ/n . We have performed some experiments to check this. The results are shown in Table II and in Fig. 4. From Table II we see that the voltage enhancement is about the same for different series of pulses if the sum of the width of the individual pulses is kept constant. A similar result can be seen from Fig. 4. Here the crosses mark the data points obtained by single pulses with the width τ up to $\tau = 10$ msec, the maximum width produced by the generator. Above 10 msec the crosses indicate results obtained with more than one 10-msec pulse. The circles are obtained with different series of pulses of 1-msec width such that the sum of the pulses in a series yields the total width τ . Again, in Fig. 4 the two sets of data are very close to each other.

Assuming that a laminar flux structure is formed by the current pulse we expect a linear relation between the flux-flow velocity v_0 during the current pulse and the inverse half-time, $(\tau^*)^{-1}$. The velocity v_0 during the current pulse can simply be varied by varying the magnetic field. We have calculated the flux-flow velocity during the beginning of the current pulse in the following way. From the linear region in the voltage-current curves obtained for small measuring currents I (less than a few hundred

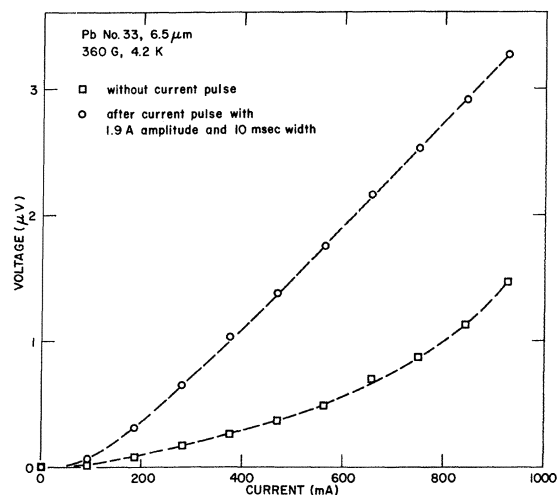


FIG. 2. Resistive voltage without and after a current pulse versus measuring current.

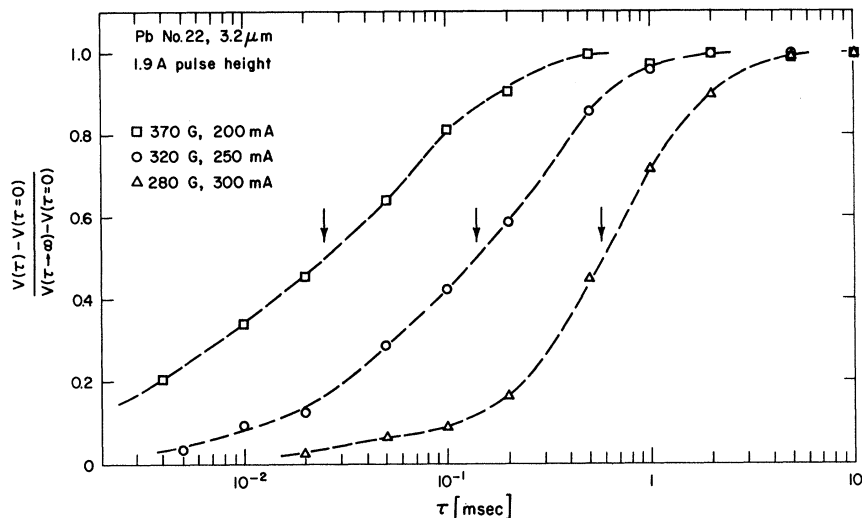


FIG. 3. Differences of the voltage after and before a pulse of 1.9-A amplitude divided by the voltage difference for a very long pulse plotted logarithmically versus the pulse width for different magnetic fields. The values of the measuring current are indicated.

mA) before the current pulse we found $v_\phi(I)$ from the relation

$$\text{grad } V = \vec{v}_\phi \times \vec{B}. \quad (1)$$

The flux-flow velocity v_ϕ at the current pulse was then obtained by extrapolating the linear relation between v_ϕ and I , found for small currents, linearly to the high current of the pulse. In making this extrapolation, we have kept in mind that the voltages obtained without a current pulse (squares in Fig. 2) are predominantly due to flux flow only in the linear region for low currents. Presumably, at high currents the flux structure rearranges itself leading to increasing voltage contributions from Ohmic resistance in the normal regions. If no rearrangement of the flux structure would be caused by the current, we would expect the voltage-current curves to be linear extensions of the linear branches found for low currents. It is therefore this linearly extended curve from which one should obtain the velocity v_ϕ at high currents.

In Fig. 5, v_ϕ at the current pulse is plotted versus

TABLE II. Voltage enhancement for different series of pulses for sample No. 36 and 1.9-A pulse height.

H (G)	Measuring current (mA)	Number of applied pulses \times pulse width (msec)	Voltage enhancement (μV)
320	300	1×3	0.21
320	300	3×1	0.21
320	300	6×0.5	0.18
320	300	(15×10)	(0.40)
380	140	1×0.25	0.31
380	140	2×0.125	0.30
380	140	5×0.05	0.26
380	140	(1×10)	(0.54)

the inverse half-time $(\tau^*)^{-1}$ for two specimens. The variation of v_ϕ was achieved, of course, through the variation in the magnetic field. The different field values in gauss are listed at each data point. We see from Fig. 5 that a linear relation between v_ϕ and $(\tau^*)^{-1}$ is, indeed, obtained. The linearity of the data in Fig. 5 is perhaps the best justification of our extrapolation procedure for obtaining v_ϕ . Similar results were found with samples No. 33, 33A, and 35.

So far we have given only a phenomenological description of the current pulse effect. In a more quantitative interpretation we would like to relate the distance $v_\phi \times \tau^*$ to the magnetic flux structure of the sample. Unfortunately, a detailed model for the development of the laminar flux structure^{6,9} at

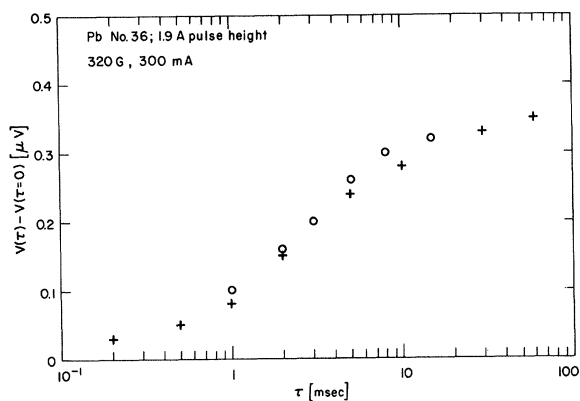


FIG. 4. Difference of the voltage after and before applying one or several current pulses of 1.9-A amplitude plotted logarithmically versus the total pulse width. Crosses: single pulse with the width indicated by τ (for $\tau \leq 10$ msec). Circles: several pulses of 1-msec width the sum of which yielding the width τ .

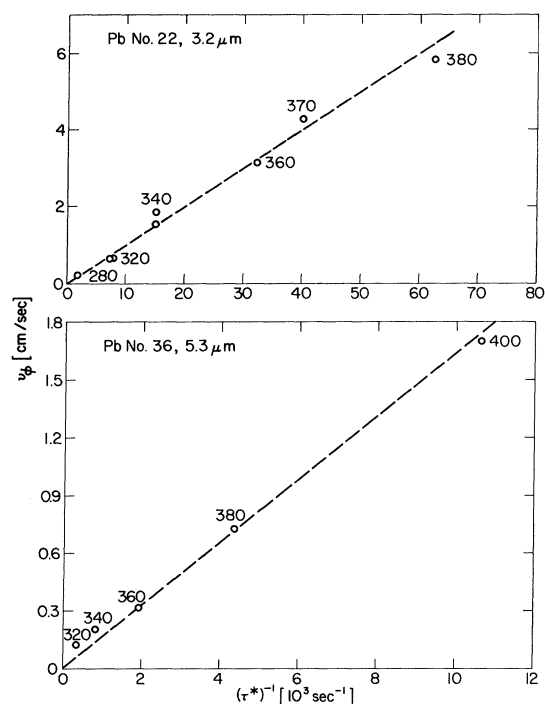


FIG. 5. Flux-flow velocity v_{ϕ} estimated for the beginning of the current pulse versus the inverse half-time $(\tau^*)^{-1}$. The number at each datum point indicates the magnetic field in gauss.

high-current densities is not yet available. Presumably, before the high-current pulse the flux structure in the Pb films consists of normal regions (flux tubes) distributed randomly in a superconducting environment.⁶ Clearly, for setting up a laminar flux structure perpendicular to the current, the current induced flux-tube motion must have a *component parallel or antiparallel to the current direction*.

The experiments of Solomon,⁶ using the diamagnetic powder technique and relatively thick superconducting plates, indicate that, depending on the magnetic field, the laminar flux structure may exist only during the current flow and may change into a meshlike pattern after the high current is turned off. It is likely that in our thin films flux pinning is strong enough for the laminae to remain unchanged

after the current pulse. Clearly, for a definite answer regarding the flux pattern the magnetic structure should be observed directly.^{13,14}

In the last column of Table I we have listed the values for the slope of the curves such as shown in Fig. 5, i. e., the product $v_{\phi} \times \tau^*$ for the different samples. We see that the length $v_{\phi} \times \tau^*$ increases monotonically with increasing film thickness. This dependence on film thickness seems reasonable, since the periodicity length of the laminar flux structure is expected to increase with increasing film thickness, thus leading to larger travel distances in the flux rearrangement for the thicker films.

It is interesting to compare the length $v_{\phi} \times \tau^*$ with theoretical models of the intermediate state flux structure, i. e., those of Landau.^{15,16} In Landau's nonbranching model¹⁵ the periodicity length in the intermediate state is given by

$$a = [d \times \Delta / \Psi_1(h)]^{1/2}. \quad (2)$$

Here d is the film thickness and Δ the surface-energy parameter. The function $\Psi_1(h)$ has been tabulated by Haenssler and Rinderer.⁹ For $d = 3 \mu\text{m}$, $\Delta \approx 400 \text{ \AA}$, and $\Psi_1(h) \approx 0.02$ we find from Eq. (2) that $a = 2.4 \mu\text{m}$. Landau's branching model¹⁶ yields for the periodicity length of the laminar structure

$$a = [d^2 \times \Delta / 1.46(1 - h^2)h]^{1/3}, \quad (3)$$

where h is the reduced magnetic field. For $d = 3 \mu\text{m}$ and $h = 0.8$ we obtain from Eq. (3) $a = 2 \mu\text{m}$. We see that the values $v_{\phi} \times \tau^*$ of Table I are close to Landau's predictions, Eqs. (2) and (3), i. e., close to the expected periodicity length of the laminar flux structure. This seems to indicate, that during formation of the laminar structure, the flux-flow velocity component parallel to the current has the same order of magnitude as the velocity perpendicular to the current which we have estimated from the longitudinal voltage and Eq. (1). However, we should keep in mind the uncertainty in v_{ϕ} at the current pulse resulting from the extrapolation to the high currents. An additional uncertainty arises from the fact that in calculating v_{ϕ} we did not take into account any voltage contribution coming directly from the Ohmic resistance in the normal regions. Because of these reasons, v_{ϕ} is perhaps not more accurate than within a factor of, say, 2-3.

*Based on work performed under the auspices of the U. S. Atomic Energy Commission.

¹P. R. Solomon and F. A. Otter, Jr., Phys. Rev. **164**, 608 (1967).

²V. A. Rowe and R. P. Huebener (unpublished).

³R. P. Huebener and A. Seher, Phys. Rev. **181**, 710 (1969).

⁴V. A. Rowe and R. P. Huebener, Phys. Rev. **185**, 666 (1969).

⁵P. R. Solomon, Phys. Rev. Letters **16**, 50 (1966).

⁶P. R. Solomon, Phys. Rev. **179**, 475 (1969).

⁷H. Träuble and U. Essmann, Phys. Status Solidi **25**, 395 (1968).

⁸G. J. Van Gorp, Phys. Rev. **178**, 650 (1969).

⁹F. Haenssler and L. Rinderer, Helv. Phys. Acta **40**, 659 (1967).

¹⁰E. R. Andrew, Proc. Roy. Soc. (London) **194**, 80 (1948).

¹¹R. P. Huebener and V. A. Rowe, Phys. Status Solidi **35**, K21 (1969).

¹²G. D. Cody and R. E. Miller, Phys. Rev. **173**, 481 (1968).

¹³H. Träuble and U. Essmann, Phys. Status Solidi **20**, 95 (1967).

¹⁴H. Kirchner, Phys. Letters **26A**, 651 (1968).

¹⁵L. D. Landau, Zh. Eksperim. i Teor. Fiz. **7**, 371 (1937).

¹⁶L. D. Landau, J. Phys. (USSR) **7**, 99 (1943).

Bulk Upper Critical Field of Clean Type-II Superconductors: V and Nb

S. J. Williamson*

Science Center, North American Rockwell Corporation, Thousand Oaks, California 91360

(Received 5 June 1970)

The bulk upper critical field H_{c2} of single crystals of Nb and V has been measured for various crystallographic orientations within the temperature range between the respective critical temperature and $T \approx 0.06^\circ\text{K}$. The normalized critical field averaged over all crystallographic directions $\langle h(t) \rangle = \langle H_{c2}(t) \rangle / (-dH_{c2}/dt)_{t=1}$, where $t = T/T_c$, and the relative anisotropy of H_{c2} for the two metals are found to be similar. The measurements support predictions of the Hohenberg-Werthamer calculation that attributes the observed anisotropy of H_{c2} to the effects of an anisotropic Fermi surface. Some differences in the behavior of $H_{c2}(t)$ for the present samples can be understood qualitatively to arise from the effects of a shorter electron-collision time τ for the less pure V specimen. At very low temperatures, $H_{c2}(0) - H_{c2}(t)$ for V does not follow a $t^2 \ln(t)$ temperature dependence, previously observed for Nb, but can be characterized by an empirical formula $t^2 \ln(t + \alpha)$ in which the constant α is conjectured to be inversely proportional to τ .

I. INTRODUCTION

The characteristics of superconductivity in Nb and V have attracted considerable interest because these metals (and possibly La¹) are the only known elemental superconductors which are type II for all temperatures below their respective transition temperatures. Therefore, pure samples have to date provided the largest ratio of electron mean free path to coherence length l/ξ_0 for a type-II system and are consequently important for testing the validity of "clean-limit" theories. Discovery by Tilley *et al.*² that H_{c2} of Nb is anisotropic demonstrated that $H_{c2}(T)$ in the clean limit may reflect "real-metal" effects not included in the Ginzburg-Landau-Abrikosov-Gor'kov (GLAG) theory which has been so successful in describing the superconducting characteristics of alloys.³ Qualitative agreement between the data of Reed *et al.*⁴ for the anisotropy of H_{c2} of pure Nb and predictions for the temperature dependence near T_c as developed in the calculations by Hohenberg and Werthamer⁵ (hereafter, HW) for the effects of Fermi-surface anisotropy suggested that the previously observed discrepancy⁶⁻¹³ between the critical field at low temperatures and that predicted by the Helfand-Werthamer¹⁴ exact solution to the GLAG theory may also arise from such real-metal effects. The possible importance of Fermi-surface effects on H_{c2} of Nb was first established on a quantitative basis by Mattheiss¹⁵ who evaluated the HW expression for the normalized

and crystallographically averaged critical field at zero temperature,

$$\langle h(0) \rangle = - \langle H_{c2}(0) \rangle / H'_{c2}(1),$$

where

$$H'_{c2}(1) = \left(\frac{dH_{c2}}{dt} \right)_{t=1}$$

and $t = T/T_c$. Employing an augmented-plane-wave (APW) band model for Nb, Mattheiss's calculations indicated that $\langle h(0) \rangle$ should be enhanced $\sim 30\%$ over the value given by the free-electron model. The predicted value of $\langle h(0) \rangle = 0.99$ was in good agreement with the experimental value of 0.96 ± 0.03 reported by Williamson and Valby.¹⁶ Thus, the first quantitative test of the nonlocal theory showed that the two-band model,¹⁷ which includes effects of coupling between s - and d -band electrons, need not be invoked to explain the observed $\langle h(0) \rangle$.

In this paper, I report the results of measurements of the temperature dependence and anisotropy of H_{c2} for single crystals of V and compare them with the behavior observed for Nb. Since V shares the same column of the periodic table as Nb and since certain aspects of the topology of the Fermi-surfaces for the two metals are reported from magnetoresistance studies¹⁸ to be similar, it might be expected that the Fermi surfaces exhibit similar anisotropy and thus a similar behavior of the normalized superconducting properties such as $\langle h(t) \rangle$ and the relative anisotropy of $H_{c2}(t)$.